


Dear Author,

Please, note that changes made to the HTML content will be added to the article before publication, but are not reflected in this PDF.

Note also that this file should not be used for submitting corrections.

**AUTHOR QUERY FORM**

 <b>ELSEVIER</b>	<b>Journal: POWER</b>  <b>Article Number: 20980</b>	<b>Please e-mail your responses and any corrections to:</b>  <b>E-mail: <a href="mailto:corrections.esco@elsevier.tnq.co.in">corrections.esco@elsevier.tnq.co.in</a></b>
--	---	--

Dear Author,

Please check your proof carefully and mark all corrections at the appropriate place in the proof (e.g., by using on-screen annotation in the PDF file) or compile them in a separate list. Note: if you opt to annotate the file with software other than Adobe Reader then please also highlight the appropriate place in the PDF file. To ensure fast publication of your paper please return your corrections within 48 hours.

For correction or revision of any artwork, please consult <http://www.elsevier.com/artworkinstructions>.

Any queries or remarks that have arisen during the processing of your manuscript are listed below and highlighted by flags in the proof.

<b>Location in article</b>	<b>Query / Remark: Click on the Q link to find the query's location in text Please insert your reply or correction at the corresponding line in the proof</b>
<b>Q1</b>	Please check the journal title in ref. [23].
<b>Q2</b>	Please confirm that given names and surnames have been identified correctly.
<b>Q3</b>	Your article is registered as a regular item and is being processed for inclusion in a regular issue of the journal. If this is NOT correct and your article belongs to a Special Issue/Collection please contact <a href="mailto:a.rassette@elsevier.com">a.rassette@elsevier.com</a> immediately prior to returning your corrections. <div data-bbox="304 1266 895 1442" style="border: 1px solid black; padding: 5px; margin-top: 10px;"> <p style="color: red;">Please check this box or indicate your approval if you have no corrections to make to the PDF file</p> <div style="display: inline-block; border: 1px solid black; width: 40px; height: 30px; vertical-align: middle;"></div> </div>

Thank you for your assistance.



Contents lists available at ScienceDirect

Journal of Power Sources

journal homepage: [www.elsevier.com/locate/jpowsour](http://www.elsevier.com/locate/jpowsour)

# Fuel blends: Enhanced electro-oxidation of formic acid in its blend with methanol at platinum nanoparticles modified glassy carbon electrodes

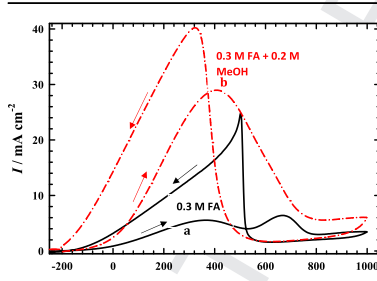
Mohamed S. El-Deab<sup>\*</sup>, Gumaa A. El-Nagar, Ahmad M. Mohammad, Bahgat E. El-Anadoulj

Department of Chemistry, Faculty of Science, Cairo University, Cairo, Egypt

## HIGHLIGHTS

- FA electrooxidation is facilitated in the presence of MeOH at nano-Pt/GC electrode.
- A shift of the onset potential and increase of oxidation current are observed.
- MeOH impedes the dehydration pathway of FA oxidation (less CO is produced).
- FA/MeOH blend is a promising fuel system in terms of fuel utilization.

## GRAPHICAL ABSTRACT



## ARTICLE INFO

### Article history:

Received 31 December 2014

Received in revised form

24 March 2015

Accepted 2 April 2015

Available online xxx

### Keywords:

Fuel utilization

Catalytic enhancement

Platinum nanoparticles

Electrocatalysis

Carbon monoxide tolerance

## ABSTRACT

The current study addresses, for the first time, the enhanced direct electro-oxidation of formic acid (FA) at platinum-nanoparticles modified glassy carbon (nano-Pt/GC) electrode in the presence of methanol (MeOH) as a blending fuel. This enhancement is probed by: (i) the increase of the direct oxidation current of FA to CO<sub>2</sub> ( $J_p^d$ , dehydrogenation pathway), (ii) suppressing the dehydration pathway ( $J_p^{ind}$ , producing the poisoning intermediate CO) and (iii) a favorable negative shift of the onset potential of  $J_p^d$  with increasing the mole fraction of MeOH in the blend. Furthermore, the charge of the direct FA oxidation in 0.3 M FA + 0.3 M MeOH blend is by 14 and 21 times higher than that observed for 0.3 M FA and 0.3 M MeOH, respectively. MeOH is believed to adsorb at the Pt surface sites and thus disfavor the “non-faradaic” dissociation of FA (which produces the poisoning CO intermediate), i.e., MeOH induces a high CO tolerance of the Pt catalyst. The enhanced oxidation activity indicates that FA/MeOH blend is a promising fuel system.

© 2015 Published by Elsevier B.V.

## 1. Introduction

Polymer electrolyte membrane fuel cells (PEMFC) are clean, highly efficient and easy-operating energy conversion devices. Methanol (MeOH) and formic acid (FA) are among the most

extensively investigated organic fuels in PEMFCs. Each fuel has its own advantages and disadvantages. For instance, the disadvantages of MeOH include its toxicity and high crossover through the Nafion<sup>®</sup> membrane (separating the fuel cell compartments) in addition to the slow oxidation kinetics, the complications associated with water management and the generation of several poisoning intermediates. On the other hand, FA has a low crossover rate and a high theoretical open circuit potential (1.45 V), but a low

<sup>\*</sup> Corresponding author.

E-mail address: [msaada68@yahoo.com](mailto:msaada68@yahoo.com) (M.S. El-Deab).

power density compared with MeOH [1–11]. The electrooxidation of FA and MeOH encounters a major drawback which is the generation of incompletely oxidized carbonaceous intermediates (e.g., CO). These intermediates are adsorbed at the surface of the catalyst leading ultimately to deterioration of its catalytic activity [1–11].

It has been shown that the oxidation of FA on platinum (Pt) and Pt-based catalysts follows a dual pathway mechanism [9,10] in which the direct oxidation of FA to CO<sub>2</sub> proceeds at a relatively low anodic potential (desired pathway, with formate anion as the reactive intermediate [12–19]). The second pathway of FA oxidation involves the oxidation of poisoning CO intermediate (resulting from the “non-faradaic” dissociation of FA) at a relatively higher anodic potential [12–19]. The accumulation of the adsorbed CO (CO<sub>ads</sub>) at the Pt catalysts causes a significant deterioration of its electrocatalytic activity [12–19].

Now an important question arises: What about the use of MeOH and FA mixture as a fuel blend? Does this blend incorporate the advantages of each component while exclude/minimize their disadvantages? This is a crucial issue which motivated us to investigate the use of a mixture of the two fuels.

Herein, the electrooxidation of a fuel blend composed of FA and MeOH (in various molar ratios) is investigated at Pt nanoparticles modified glassy carbon (nano-Pt/GC) electrode. Cyclic voltammetry (CV) and CO stripping experiments are used to evaluate the electrocatalytic activity of the catalyst under various operating conditions aiming at maximizing the fuel utilization.

## 2. Experimental

Glassy carbon (GC, d = 3.0 mm) and polycrystalline (Pt, d = 1.6 mm) electrodes served as the working electrodes. An Ag/AgCl/KCl (sat.) and a spiral Pt wire are used as reference and counter electrodes, respectively. Conventional procedure is applied to clean the Pt and GC electrodes as described elsewhere [12,19]. While, the electrodeposition of nano-Pt on GC electrode is carried out in 0.1 M H<sub>2</sub>SO<sub>4</sub> containing 1.0 mM H<sub>2</sub>[PtCl<sub>6</sub>] solution via a potential step electrolysis from 1 to 0.1 V for 300 s (resulting in a loading of 65 μg Pt) as estimated from the charge of the *I-t* curve recorded during the potentiostatic electrolysis at 0.1 V. The electrocatalytic activity of the GC modified electrodes with nano-Pt toward FAO is examined in an aqueous solution of 0.3 M FA (with pH~3.5). The pH is adjusted to 3.5 by adding a proper amount of 0.1 M NaOH. At this pH an appreciable amount of FA is ionized to formate anion (about one third). This would enhance the ionic conductivity in the solution, thus reduces the polarization resistance, in addition to compressing the thickness of the diffusion layer. Moreover, Osawa et al. [13,14] have studied the effect of pH on FAO at Pt/C anodes and found that FAO current has a volcano increase with pH showing a maximum current at pH = pK<sub>a</sub> of FA (≅ 3.5). CV is performed in a conventional two-compartment three-electrode glass cell. All measurements are performed at room temperature (25 ± 1 °C) using an EG&G potentiostat (model 273A) operated with Echem 270 software. A field emission scanning electron microscope, FE-SEM, (QUANTA FEG 250) coupled with an energy dispersive X-ray spectrometer (EDX) unit is employed to evaluate the electrode's morphology and surface composition. Current densities are calculated on the basis of the geometric surface area of the working electrodes.

## 3. Results and discussions

### 3.1. Material and electrochemical characterizations

Fig. 1A shows an SEM micrograph for nano-Pt/GC electrode, in which nano-Pt with an average particle size of 80 nm are

homogeneously covering the entire GC surface. The effort is committed next to evaluate the composition and crystal structure of the electrode involved in this investigation. The XRD investigation reveals the deposition of nano-Pt in a face-centered cubic (fcc) structure (Fig. 1B), where all the typical characteristic peaks of Pt (1 1 0), (2 0 0) and (2 2 0) appeared. The three peak appeared at 2θ = 25°, 43° and 78.8° are associated to the carbon support (0 0 2), (1 0 1) and (1 1 0), respectively. On the other hand, EDX spectral analysis provides a direct evidence for the successful electrodeposition of nano-Pt onto the surface of GC (Fig. 1C). Moreover, a typical characteristic CV for a Pt substrate is observed in 0.5 M H<sub>2</sub>SO<sub>4</sub> at nano-Pt/GC electrode in which a broad oxidation peak for the Pt-oxide formation (commences at ca. 0.65 V and extends up to 1.4 V) coupled with a single reduction peak centered at ca. 0.45 V (Fig. 1D), in addition to hydrogen adsorption/desorption (H<sub>ads/des</sub>) couple appeared in the potential region from -0.2 to 0.2 V for the nano-Pt/GC electrode.

### 3.2. Electrocatalytic activity towards FA oxidation

Fig. 2 (A–C) shows CVs obtained at nano-Pt/GC electrode in aqueous solutions (pH 3.5) containing (A) 0.3 M FA, (B) 0.3 M MeOH and (C) 0.3 M FA + 0.2 M MeOH (1:0.66 molar ratio) at a potential scan rate of 0.1 V s<sup>-1</sup>. A typical CV of FAO at Pt surface is obtained (Fig. 2A) with the appearance of two oxidation peaks in the forward scan, at ca. 0.3 V (assigned to the direct oxidation of FA to CO<sub>2</sub>, I<sub>p</sub><sup>d</sup>) and at ca. 0.7 V (assigned to the oxidation of the poisonous CO<sub>ads</sub> species to CO<sub>2</sub>, I<sub>p</sub><sup>ind</sup>) [12–19]. The CO<sub>ads</sub> refers to the adsorbed CO resulted from the “non-faradaic” dissociation of FA. At low potential (ca. 0.3 V), the measured current corresponds to FAO at Pt sites via the dehydrogenation pathway. At high potential (ca. 0.7 V), the CO<sub>ads</sub> is oxidized by Pt-OH, which releases most Pt sites for FAO. The relative peak current intensities indicate the level of Pt surface poisoning by CO<sub>ads</sub>. In the backward cathodic-going scan, most of the poisonous intermediates have been released to expose a clean Pt surface for FAO through the dehydrogenation pathway. Therefore, the current intensity in the backward scan increases largely (peak I<sub>b</sub> in Fig. 2A). On the other hand, typical CV of MeOH oxidation reaction (MOR) at nano-Pt/GC electrode is obtained (Fig. 2B), where one oxidation peak appeared at ca. -0.1 V corresponding to MOR.

Interestingly, the use of fuel blend composed of 0.3 M FA and 0.3 M MeOH results in a large increase in the direct FAO peak current (I<sub>p</sub><sup>d</sup>) with a concurrent vanishing of the indirect FAO peak (dehydration pathway, poisoning pathway), i.e., FA is exclusively oxidized via the dehydrogenation pathway (see Fig. 2C). The significant increase of I<sub>p</sub><sup>d</sup> at the expense of I<sub>p</sub><sup>ind</sup> indicates that less amount of CO<sub>ads</sub> is produced in the presence of MeOH. The ratio I<sub>p</sub><sup>d</sup>/I<sub>b</sub>, with I<sub>b</sub> refers to backward oxidation current, is a useful index for the catalytic tolerance of the electrode against the formation of carbonaceous species. A low I<sub>p</sub><sup>d</sup>/I<sub>b</sub> ratio indicates poor oxidation of FA to CO<sub>2</sub> and excess accumulation of carbonaceous species at the electrode surface. This ratio increases from 0.2 to ca. 0.8 for FAO at nano-Pt/GC electrode in pure FA (0.3 M FA, Fig. 2A) and fuel blend (0.3 M FA + 0.3 M MeOH, Fig. 2C), respectively, which is by 4 times higher. Again, this supports our conclusion (by comparing I<sub>p</sub><sup>d</sup> and I<sub>p</sub><sup>ind</sup>) that less amount of CO<sub>ads</sub> is produced in the forward scan for the fuel blend than pure fuel at the nano-Pt/GC electrode. The use of FA/MeOH blend as a fuel could stimulate a higher degree of reversibility and catalytic activity towards FAO, a feature that is always desirable in fuel cells manufacturing.

Moreover, Fig. 3 (A–C) shows CVs obtained at nano-Pt/GC electrode in 0.5 M H<sub>2</sub>SO<sub>4</sub> containing (A) 0.3 M FA, (B) 0.3 M MeOH and (C) 0.3 M FA + 0.3 M MeOH (1:1 molar ratio) measured at 0.1 V s<sup>-1</sup>. This figure shows the same behavior of the enhancing

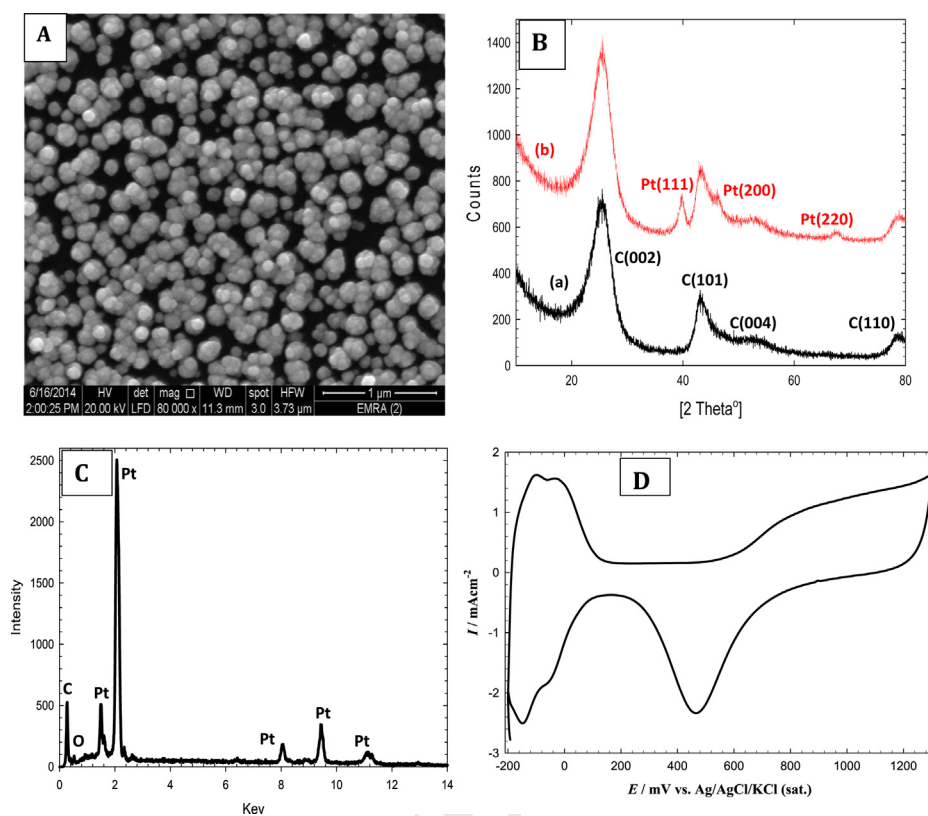


**Fig. 1.** (A) FE-SEM image of nano-Pt/GC surface, (B) XRD pattern of (a) GC and (b) nano-Pt/GC electrodes, (C) EDX analysis of nano-Pt/GC electrode and (D) CV obtained at nano-Pt/GC electrode in 0.5 M  $\text{H}_2\text{SO}_4$ . Potential scan rate:  $0.1 \text{ V s}^{-1}$ .

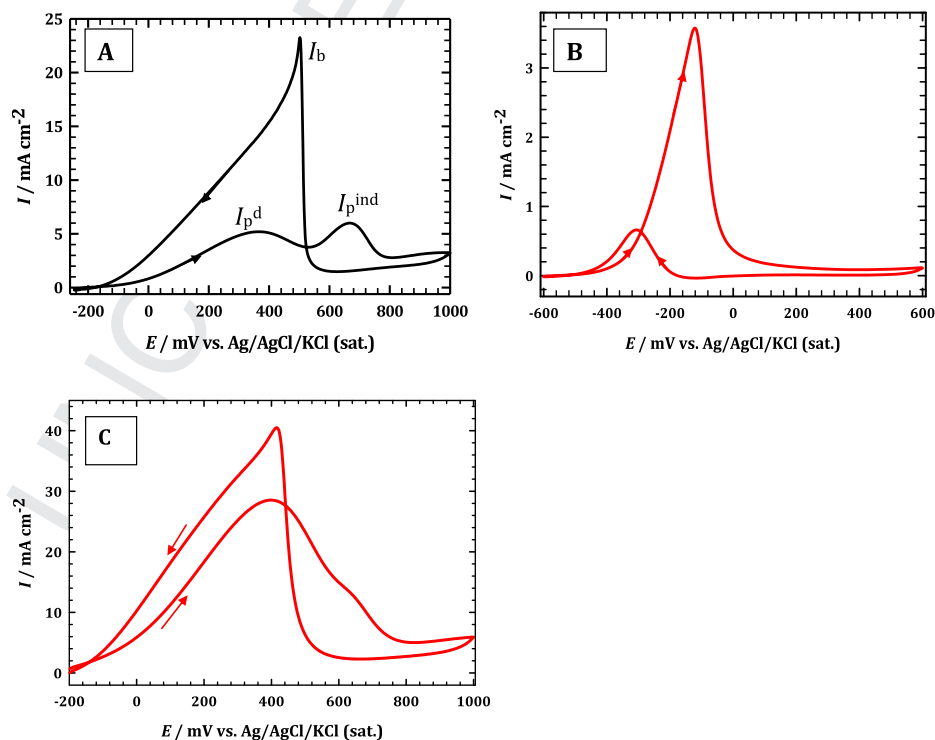


**Fig. 2.** CVs obtained at nano-Pt/GC electrode in aqueous solutions (pH 3.5) containing (A) 0.3 M FA, (B) 0.3 M MeOH and (C) 0.3 M FA + 0.2 M MeOH (1:0.67 molar ratio). Potential scan rate:  $0.1 \text{ V s}^{-1}$ .

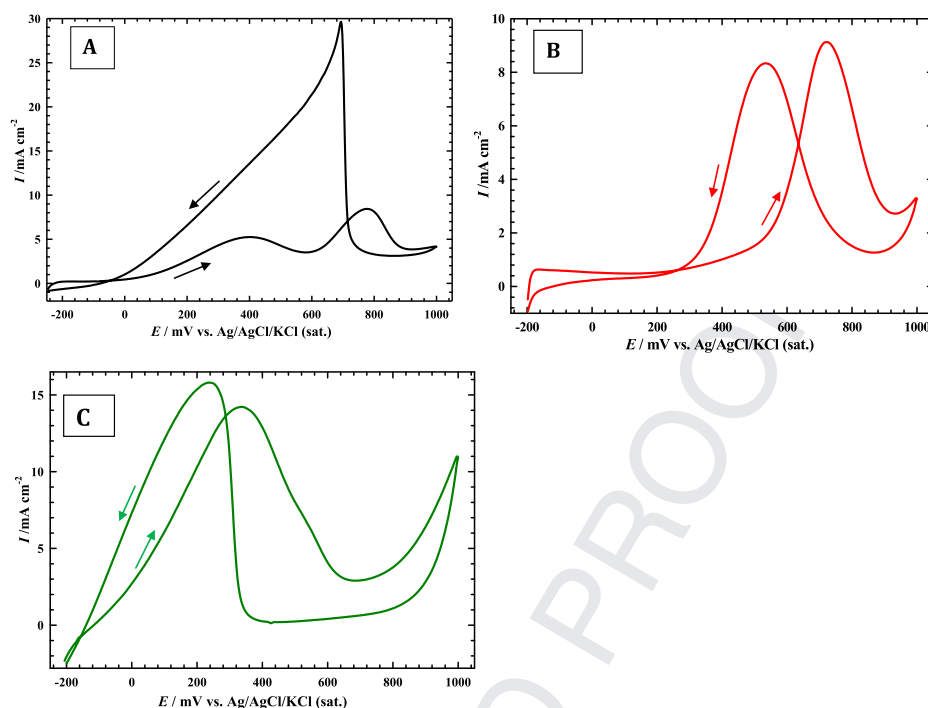


Fig. 3. CVs obtained at nano-Pt/GC electrode in 0.5 M H<sub>2</sub>SO<sub>4</sub> containing (A) 0.3 M FA, (B) 0.3 M MeOH and (C) 0.3 M FA + 0.3 M MeOH (1:1 molar ratio). Potential scan rate: 0.1 V s<sup>-1</sup>.

effect of MeOH on FAO as that obtained at pH 3.5 (refer to Fig. 2A–C). That is a significant enhancement in the direct FAO ( $J_p^d$ ) at the expense of  $J_p^{ind}$  is obtained.

The electrocatalytic activity of the nano-Pt/GC electrode towards FAO in FA/MeOH fuel blends with various MeOH molar ratios are presented in Fig. 4A. This figure shows that, a progressive increase in  $J_p^d$  with a concurrent depression of  $J_p^{ind}$  is observed as the concentration of MeOH increases ( $J_p^{ind}$  is completely ceased in the presence of 0.3 M MeOH). Additionally, a large negative shift in the onset potential of the direct FAO is observed. Moreover, further increase of MeOH concentration results in the appearance of three peaks in the positive-going potential scan, namely at  $-0.1$  V (attributed to MOR), 0.3 V (referred to  $J_p^d$ ) and 0.7 V (referred to  $J_p^{ind}$ ) see Fig. 4B (curve a). MOR peak at  $-0.1$  V increases with further increase in MeOH concentration with a supervising disappearance of the two oxidation peaks of FA in the presence of 0.3 M FA together with [MeOH]  $\geq$  0.5 M (see Fig. 4B (curve b)).

Two parameters are introduced to evaluate the enhancing effect associated with the use of FA/MeOH as a fuel blend, namely, fuel utilization ( $FU = Q^*/C_F$ ) and the enhancement factor ( $EF = Q^*/Q_d$ ). Note that  $Q^*$  and  $Q_d$  refer to the charge of direct FAO in FA/MeOH blend and in pure FA solution, respectively, and  $C_F$  is the total concentration of the two fuels in a certain blend.  $FU$  probes the amount of charge consumed during the oxidation process per mole of fuel. The increase of  $FU$  indicates better performance for the catalyst towards the fuel oxidation (higher oxidation capacity). Fig. 5A depicts that a volcano-shape increase of  $FU$  with MeOH mole fraction ( $x$ ) reaching a maximum value at  $x = 0.5$ . Further increase in  $x > 0.5$  results in a decrease in  $FU$  reaching a minimum value at  $x = 1.0$  (pure MeOH as a fuel). The observed behavior might originate from retarding/reducing the amount of CO<sub>ads</sub> and/or catalyzing its oxidation at the designed potential range of  $Q^*$ , in the presence of MeOH at  $x < 0.5$ , and thus favoring the dehydrogenation pathway. At higher  $x$ ,  $FU$  decreases due to blockage of the Pt active sites available for direct FAO by MeOH. This observation

points to the crucial role of the blending component (MeOH) as an inhibitor for the non-faradaic dissociation of FA (resulting in the formation of the poisoning CO<sub>ads</sub> (cf. Fig. 6A)). That is, the use of FA/MeOH (with  $x = 0.5$ ) results in a facile oxidation of FA at nano-Pt/GC electrode by about 7 and 11 times higher  $FU$  compared to using pure FA and pure MeOH, respectively.

The second parameter is the enhancement factor ( $EF = Q^*/Q_d$ ). It is a ratio which probes the degree of the catalytic enhancement of nano-Pt/GC electrode towards direct FAO upon the addition of MeOH. Fig. 5B reveals that,  $EF$  increases with  $x$  in a similar fashion to that observed for  $FU$ . A quick overview of Fig. 5A and B reveals that the use of equimolar amounts of FA and MeOH is the best blend composition with the maximum  $FU$  and  $EF$ .

In order to verify the catalytic enhancement of the direct FAO in the presence of MeOH, a controlled CO stripping experiment is conducted at nano-Pt/GC electrode with a pre-adsorbed CO (which is in-situ generated via the “non-faradaic” dissociation of FA, at open circuit potential, in its blend with MeOH with various molar ratios). The oxidative stripping of CO is shown in Fig. 6A. This figure indicates that a systematic lowering in the intensity of the oxidation peak current of CO is observed by increasing the MeOH molar ratio. This finding provides an evidence for the assumption that MeOH (as a blending fuel) prevents/impedes the formation of CO but not significantly enhancing its oxidative removal.

In the same context, and in order to find a plausible explanation for the observed behavior, the influence of MeOH on the work function of the Pt catalyst is considered. That is, it has been shown that the polarizing potential of a certain electrode is related to changes in the catalyst work function ( $\Phi$ ).  $\Phi$  is sensitive to any physicochemical changes on the electrode surface and is strongly affected by the conditions of the surface of the catalyst. That is the presence of minute amounts of contaminant (less than a monolayer) can change the work function substantially and in turn the catalytic activity of the catalyst may change [20,21]. This is a result of the formation of electric dipoles at the surface, resulting in the

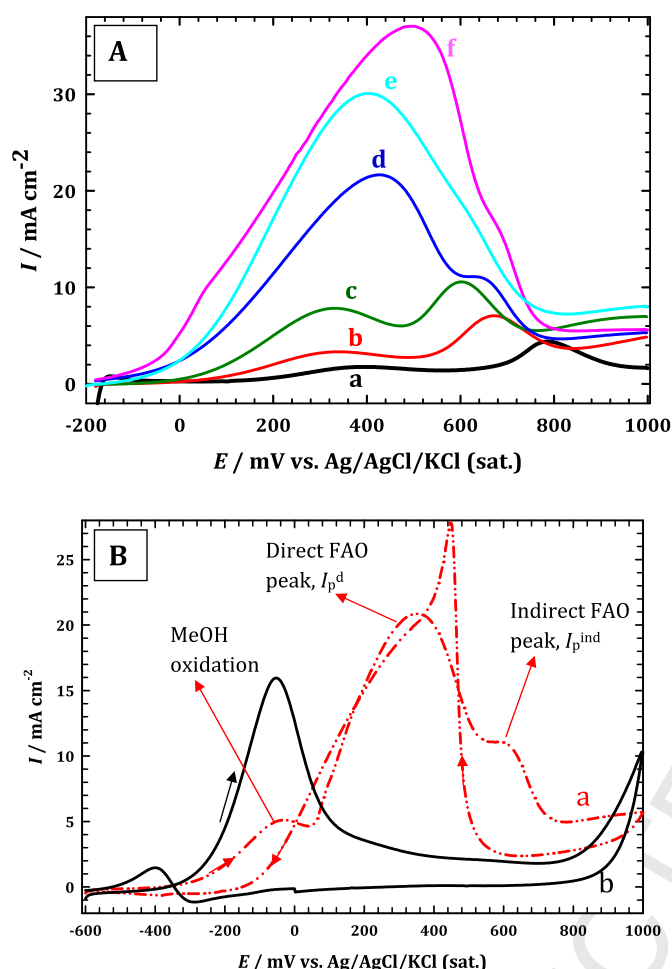


**Fig. 4.** (A) LSVs obtained at nano-Pt/GC electrode in aqueous solutions (pH 3.5) containing 0.3 M FA and various molar ratios of MeOH: (a) 1:0, (b) 1:0.003, (c) 1:0.03, (d) 1:0.33, (e) 1:0.73 and (f) 1:1. (B) CVs obtained at nano-Pt/GC electrode in an aqueous solution (pH 3.5) containing (a) 0.3 M FA + 0.4 MeOH (1:1.33 molar ratio), and (b) 0.3 M FA + 0.5 M MeOH (1:1.67 molar ratio). Potential scan rate:  $0.1 \text{ V s}^{-1}$ .

change in the energy needed for an electron transfer from/to the surface of the catalyst. For instance, MeOH adsorption was found to cause a monotonic decrease in Pt work function down to  $-1.8 \text{ eV}$  relative to the clean surface. Thus, the observed decrease of the amount of the poisoning CO intermediate adsorbed at the nano-Pt/GC electrode (Fig. 6A) could result from a decrease in the Pt work function due to MeOH adsorption [22–26].

The stability of the nano-Pt/GC electrode towards FAO in various FA/MeOH fuel blends has been probed by measuring the  $I$ - $t$  transients at  $0.15 \text{ V}$  (presented in Fig. 6B). This figure depicts that in the absence of MeOH (curve a), the current decays rapidly due to the accumulation of the poisoning  $\text{CO}_{\text{ads}}$  on the Pt surface with a poisoning rate =  $0.06 \text{ s}^{-1}$  calculated from the following equation [27]:

$$\text{Poisoning Rate} = \frac{100}{I_0} \times \left( \frac{dI}{dt} \right)_{t > 500\text{s}} \quad (1)$$

where  $I_0$  and  $(dI/dt)_{t > 500\text{s}}$  refer to the maximum obtainable current density at  $t = 0 \text{ s}$ , and the rate of decay of current with time at  $t > 500 \text{ s}$  (i.e., in the steady-state current region), respectively.

On the contrary, in the presence of MeOH, nano-Pt/GC electrode supports a higher steady-state oxidation current which decays only

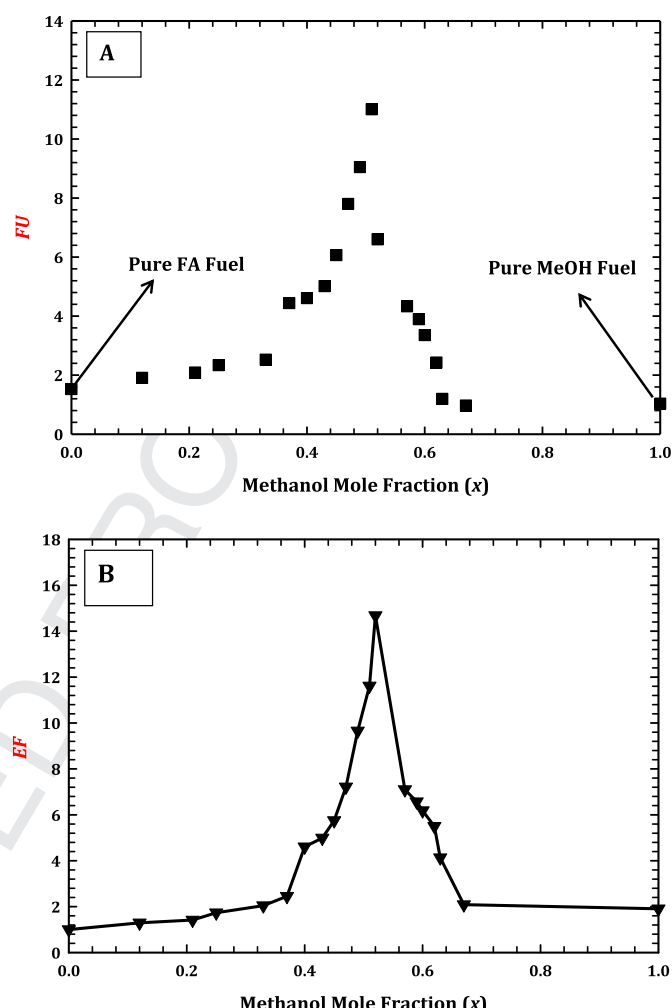


**Fig. 5.** Variation of (A) fuel utilization ( $FU = Q^*/C_F$ ) and (B) enhancement factor ( $EF = Q^*/Q_d$ ) with methanol mole fraction (x). Note that  $Q^*$  and  $Q_d$  refer to the charge of direct FAO in FA/MeOH blend and in pure FA solution, respectively, and  $C_F$  is the total concentration of the two fuels.

slightly with time, corresponding to poisoning rates of 0.02, 0.01 and  $0.005 \text{ s}^{-1}$  in the presence of 0.01, 0.1, and 0.3 M MeOH, respectively. This indicates the sustainable tolerance of the Pt catalyst against CO poisoning in the presence of MeOH, and thus FA/MeOH blend is suggested as a promising fuel for application in PEMFCs.

#### 4. Conclusions

This study revealed, for the first time, that the use of a blend of FA and MeOH resulted in significant enhancement of the direct FAO with a concurrent suppression of the poisoning CO pathway at Pt-based catalyst. The use of a blend composed of 0.3 M FA and 0.3 M MeOH (1:1 molar ratio) resulted in the best electrocatalytic activity towards FAO with a complete suppression of the indirect (poisoning) pathway of FAO at nano-Pt/GC electrode. That is MeOH is believed to retard/impede CO adsorption onto the surface of the Pt catalyst possibly due to a decrease of the work function of Pt, thus leading to progressively less amounts of CO are being adsorbed at Pt as evident from the oxidative stripping experiments measured in the presence of various molar ratios of MeOH in FA/MeOH blends. Moreover, the stability of nano-Pt/GC electrode towards FAO for a prolonged electrolysis of FA/MeOH blend is higher than

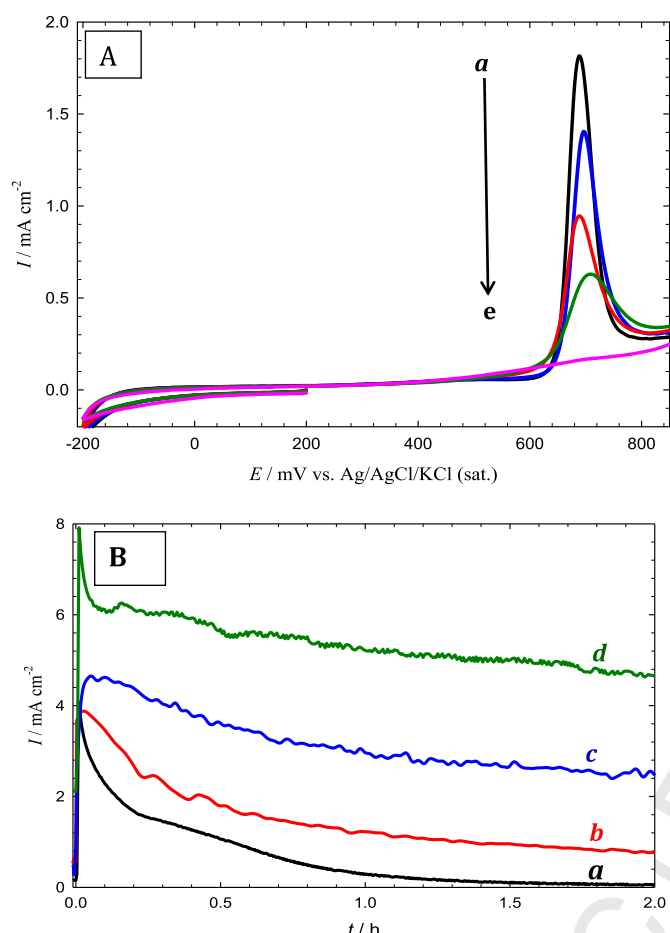


**Fig. 6.** (A) Oxidative stripping of CO at nano-Pt/GC electrode in 0.5 M Na<sub>2</sub>SO<sub>4</sub> (pH 3.5). Note that CO monolayers were formed at open circuit potential from aqueous solutions containing 0.5 M FA and various molar ratios of MeOH: (a) 1:0, (b) 1:0.2, (c) 1:0.4, (d) 1:0.6 and (e) 1:1. Potential scan rate: 0.05 V s<sup>-1</sup>. (B) *I*-*t* transients measured at a constant potential of 0.15 V at nano-Pt/GC electrode in aqueous solutions (pH 3.5) containing 0.3 M FA and various molar ratios of MeOH: (a) 1:0, (b) 1:0.03, (c) 1:0.33 and (d) 1:1.

that observed for pure FA fuel.

## References

- [1] O.Z. Sharaf, M.F. Orhan, An overview of fuel cell technology: fundamentals and applications, *Renew. Sustain. Energy Rev.* 32 (2014) 810–853.
- [2] Y. Wang, K.S. Chen, J. Mishler, S.C. Cho, X.C. Adroher, A review of polymer electrolyte membrane fuel cells: technology, applications, and needs on fundamental research, *Appl. Energy* 88 (2011) 981–1007.
- [3] C. Rice, S. Ha, R.I. Masel, P. Waszczuk, A. Wieckowski, T. Barnard, Direct formic acid fuel cells, *J. Power Sources* 111 (2002) 83–89.
- [4] X. Yu, P.G. Pickup, Recent advances in direct formic acid fuel cells (DFAFC), *J. Power Sources* 182 (2008) 124–132.

- [5] S. Wasmus, A. Klvær, Methanol oxidation and direct methanol fuel cells: a selective review, *J. Electroanal. Chem.* 461 (1999) 14–31.
- [6] G. Samjeské, A. Miki, S. Ye, M. Osawa, Mechanistic study of electrocatalytic oxidation of formic acid at platinum in acidic solution by time-resolved surface-enhanced infrared absorption spectroscopy, *J. Phys. Chem. B* 110 (2006) 16559–16566.
- [7] M. Osawa, K. Komatsu, G. Samjeské, T. Uchida, T. Ikeshoji, A. Cuesta, C. Gutierrez, The role of bridge-bonded adsorbed formate in the electrocatalytic oxidation of formic acid on platinum, *Angew. Chem. Int. Ed.* 50 (2011) 1191–1195.
- [8] J.D. Lovic, A.V. Tripkovic, S.L. Gojkovic, K.D. Popovic, D.V. Tripkovic, P. Olszewski, A. Kowal, Kinetic study of formic acid oxidation on carbon-supported platinum electrocatalyst, *J. Electroanal. Chem.* 581 (2005) 294–302.
- [9] N. Wongyao, A. Therdthianwong, S. Therdthianwong, Performance of direct alcohol fuel cells fed with mixed methanol/ethanol solutions, *Energy Convers. Manag.* 52 (2011) 2676–2681.
- [10] T.J. Leo, M.A. Raso, E. Navarro, E. Sánchez de la Blanca, M. Villanueva, B. Moreno, Response of a direct methanol fuel cell to fuel change, *Int. J. Hydrog. Energy* 35 (2010) 11642–11648.
- [11] T.J. Leo, M.A. Raso, E. Navarro, E. Mora, Long term performance study of a direct methanol fuel cell fed with alcohol blends, *Energies* 6 (2013) 282–293.
- [12] G.A. El-Nagar, A.M. Mohammad, M.S. El-Deab, B.E. El-Anadoul, Electrocatalysis by design: enhanced electrooxidation of formic acid at platinum nanoparticles–nickel oxide nanoparticles binary catalysts, *Electrochim. Acta* 94 (2013) 62–71.
- [13] J. Joo, T. Uchida, A. Cuesta, M. Koper, M. Osawa, The effect of pH on the electrocatalytic oxidation of formic acid/formate on platinum: A mechanistic study by surface-enhanced infrared spectroscopy coupled with cyclic voltammetry, *Electrochim. Acta* 129 (2014) 127–136.
- [14] J. Joo, T. Uchida, A. Cuesta, M. Koper, M. Osawa, Importance of acid–base equilibrium in electrocatalytic oxidation of formic acid on platinum, *J. Am. Chem. Soc.* 135 (2013) 9991–9994.
- [15] Y.X. Chen, M. Heinen, Z. Jusys, R.J. Behm, Kinetics and mechanism of the electrooxidation of formic acid–spectroelectrochemical studies in a flow cell, *Angew. Chem. Int. Ed.* 45 (2006) 981–985.
- [16] A. Cuesta, G. Cabello, C. Gutiérrez, M. Osawa, Adsorbed formate: the key intermediate in the oxidation of formic acid on platinum electrodes, *Phys. Chem. Chem. Phys.* 13 (2011) 20091–20095.
- [17] P. Samjeské, M. Osawa, Current oscillations during formic acid oxidation on a Pt electrode: insight into the mechanism by time-resolved IR spectroscopy, *Angew. Chem.* 117 (2005) 5840–5844.
- [18] G.A. El-Nagar, A.M. Mohammad, M.S. El-Deab, T. Ohsaka, B.E. El-Anadoul, Acrylonitrile-contamination induced enhancement of formic acid electrooxidation at platinum nanoparticles modified glassy carbon electrodes, *J. Power Sources* 265 (2014) 57–61.
- [19] G.A. El-Nagar, A.M. Mohammad, Enhanced electrocatalytic activity and stability of platinum, gold, and nickel oxide nanoparticles-based ternary catalyst for formic acid electro-oxidation, *Int. J. Hydrog. Energy* 39 (2014) 11955–11962.
- [20] M.S. El-Deab, F. Kitamura, T. Ohsaka, Impact of acrylonitrile poisoning on oxygen reduction reaction at Pt/C catalysts, *J. Power Sources* 229 (2013) 65–71.
- [21] R. Adzic, *Frontiers in electrochemistry*, in: J. Lipkowski, P.N. Ross (Eds.), *Electrocatalysis* vol. 197, Wiley-VCH, New York, NY, USA, 1998.
- [22] C.G. Vayenas, S. Bebelis, I.V. Yentekakis, H.-G. Lintz, Non-faradaic electrochemical modification of catalytic activity: a status report, *Catal. Today* 11 (1992) 303–438.
- [23] C.G. Vayenas, S. Bebelis, S. Ladas, Dependence of catalytic rates on catalyst work function, *Nature* 343 (1990) 625–627.
- [24] C.G. Vayenas, S. Bebelis, M. Despotopoulou, Non-faradaic electrochemical modification of catalytic activity 4. The use of β'-Al<sub>2</sub>O<sub>3</sub> as the solid electrolyte, *J. Catal.* 128 (1991) 415–435.
- [25] S. Trasatti, Surface science and electrochemistry: concepts and problems, *Surf. Sci.* 335 (1995) 1–9 (And the references cited therein).
- [26] W. Schmickler, The surface dipole moment of species adsorbed from a solution, *J. Electroanal. Chem.* 249 (1988) 25–33.
- [27] J. Jiang, A. Kucernak, Electrooxidation of small organic molecules on mesoporous precious metal catalysts: II: CO and methanol on platinum–ruthenium alloy, *J. Electroanal. Chem.* 543 (2003) 187–199.